Original Manuscript

JOURNAL OF COMPOSITE MATERIALS

Journal of Composite Materials
2025, Vol. 0(0) 1–11

DOI: 10.1177/00219983251329115
journals.sagepub.com/home/jcm
Sage

Mechanical characterization of granular actuators

Sophia Eristoff[1], Lina Sanchez-Botero[1] and Rebecca Kramer-Bottiglio[1]

Abstract

Phase-change granular actuators combine the high volumetric expansion and actuation stress of bulk phase-change systems with the tunable properties of granular materials. One form of these actuators utilizes microcapsule grains made from an elastic matrix encapsulating multiple solvent cores, where phase changes from liquid to gas drive volumetric expansion. Previous work demonstrated grain expansions up to 700%, though material selection was not optimized. This study explores how shell and core material choices affect the synthesis and performance of phase-change granular actuators. We identify specific combinations of solvents and silicone matrices that influence encapsulation efficiency, grain morphology, and processing requirements. Results show that increasing shell stiffness and core solvent boiling point raises actuation temperatures, while softer shells enable greater volumetric expansions. Overall, tuning the material composition allows for control of actuation metrics.

Keywords

multi-core microcapsule, double emulsion, soft robotics, phase-change actuator, multi-phase composites, granular actuator

Introduction

Granular materials, composed of discrete particle assemblies, may provide a versatile platform for dynamic material programmability due to the tunability of individual particle properties.[1] The mechanical response of granular materials depends on numerous factors, such as the arrangement of particles in the assembly,[2,3] the mass, modulus, shape, and frictional interactions of individual particles,[4] and the boundary conditions or pressure of the assembly.[5–10] Many of these variables can be adjusted by manipulating individual particles within the system. For instance, if individual particles in an assembly can change size, shape, or position, they may self-rearrange, enabling bulk property modulation. Towards this potential for self-adaptive behavior, several works have introduced active granular matter. For example, liquid crystal elastomer microparticle actuators and soft magnetic composites have been synthesized to enable thermal-responsive shape-change and motion,[11–13] and we previously introduced granular actuators—particles capable of independent volumetric expansion.[14]

Our instantiation of granular actuators is a multi-core microcapsule solution, wherein phase-changing material cores are embedded in an elastic material shell. In prior work, liquid-to-gas phase-changing cores embedded in soft silicone shells enabled grain volumetric expansions with actuation stresses comparable to other soft actuators (62 kPa) at rapid time scales (~1000 mm/sec). The phase-change granular actuators exhibited variable moduli based on assembly pressure and imparted thixotropic properties on carrier fluids to enable 3D printable actuators, which aligns with prior reporting on printable biphasic materials.[15–17]

Selecting materials for phase-change actuators, including granular actuators, involves two key considerations: (1) the matrix or shell material must be soft enough to allow for substantial volumetric expansions, and (2) the solvent must have a low-boiling-point to induce phase change without degrading the encapsulating matrix. Prior work has primarily focused on reducing the BP of the encapsulated

[1]Department of Mechanical Engineering and Materials Science, Yale University, New Haven, CT, USA

Corresponding author:
Rebecca Kramer-Bottiglio, School of Engineering and Applied Science, Yale University, New Haven, 9 Hillhouse Ave, CT, 06520, USA.
Email: rebecca.kramer@yale.edu

Data Availability Statement included at the end of the article.

solvent to make the temperature of actuation (T_A) more accessible.[18–21] However, one drawback of low-BP solvents is their tendency to evaporate easily. Solvents such as ethanol and acetone, with very low BPs, can evaporate at ambient conditions. In turn, this makes it difficult to reach the T_A prior to the encapsulated solvent evaporating. Additionally, many studies, including our own, have used Ecoflex 00-30 as the matrix material,[14,19–21] without exploring how different matrix materials might influence actuation performance. While other works have used latex-based shell materials for phase-change actuation,[22] the rationalization was not based on optimizing or tuning actuation properties but rather on preventing solvent escape. There is a clear gap in the understanding of how the choice of constituent materials impacts the performance of granular actuators, and phase-change actuators more broadly.

Research objectives

In this work, we expand on our previous research on soft phase-changing granular actuators by synthesizing new granular actuators with diverse constituent materials. We begin by investigating how different solvent and elastic matrix combinations influence key processing parameters of granular actuators, such as grain size, morphology, and encapsulation efficiency. Next, we examine the effects of the solvent and hyperelastic matrix materials on critical actuation parameters, including actuation stress, peak actuation temperature, and volumetric expansion. We find that hyperelastic matrix stiffness and encapsulated solvent boiling point have outsized impacts on actuation metrics. Finally, we demonstrate how varying the constituent materials in granular actuators can enable the synthesis of larger actuators with tunable actuation properties. This study provides a general guideline for material selection in phase-change granular actuators to achieve specific desired outcomes.

Results

Experimental variables and synthesis process

The grains undergo volumetric expansion due to the liquid-to-gas phase transition of the encapsulated solvent within the hyperelastic shell (Figure 1(a)). We explore various commercially available silicone shell materials, including Ecoflex 00-10 (EF10), Ecoflex 00-30 (EF30), and DragonSkin10 (DS10), to assess how the hyperelastic shell influences the actuation properties of the grains (Figure 1(b)). Additionally, we investigate several core solvents, some of which have been successfully employed in previously synthesized phase-change actuators, including ethanol (EtOH),[19–21] deionized water (DIW), and perfluorodecalin (PFD),[14] to generalize how the actuation properties of the grains are impacted by the encapsulated solvent properties (Figure 1(c)). The synthesis method for the granular actuators remains consistent with our prior work,[14] using a scalable double emulsion method to synthesize active grains with multiple solvent cores (Figure 1(d)). To isolate variables for testing, all grains are synthesized with a uniform volume fraction of encapsulated solvent, nominally 7 vol.%.

Effects of processing parameters

Each material used in this study has different material properties, as shown in Figures 1(b) and 1(c). Due to these differences, despite using uniform synthesis parameters (Figure 1(d)), the resultant grains vary in several ways. Figure 2(a)–(c) shows the size distribution of grains with different shell materials or solvent cores (all distributions are shown in Figure S1). The double emulsion process used to synthesize the grains can be affected by a variety of properties, including but not limited to the viscosity of the continuous phase, the viscosity of the pre-cure actuator material, the temperature of the system, and the solubility of the pre-cured actuator material in the continuous phase.[14,23] When these variables are changed, the force required to break up the material into droplets differs and will yield particles with different size distributions. Because we use different hyperelastic matrices and solvent materials throughout this study, which all have different properties, we see a change in particle size despite using the same processing parameters. Additionally, while we see normal particle size distributions for some materials, we see some skewed particle size distributions for others.

Figure 2(d) summarizes the size distributions of all of the granular actuators tested in this study. The ethanol-encapsulated EF10 and EF30 grains exhibit the smallest average measured diameter, which may be due to favorable material compatibility between the solvent and the hyperelastic resin. Emulsions are created by mixing in two immiscible phases to produce a continuous phase with many inclusions of the dispersed phase. In the double emulsion process used for this study, an emulsion of solvent and resin is first created. Thereafter, the initial emulsion is introduced into the viscous shear-thinning sodium alginate continuous phase to yield granular actuators. Material compatibility between the resin and solvent may reduce the viscosity of the mixture in the second emulsion, requiring less force for droplet break-up, yielding smaller grains. Increasing the mixing speed will also yield smaller grains.[14,23,24] We find that in general, DS10 grains seem to be the largest. This can be owed to the high viscosity of DS10, which is approximately 7X that of EF30 and almost 2X that of EF10 (see Figure 1(b)). Due to the high viscosity of DS10, a larger force is required to breakup the material into droplets, which leads to larger resulting particles.

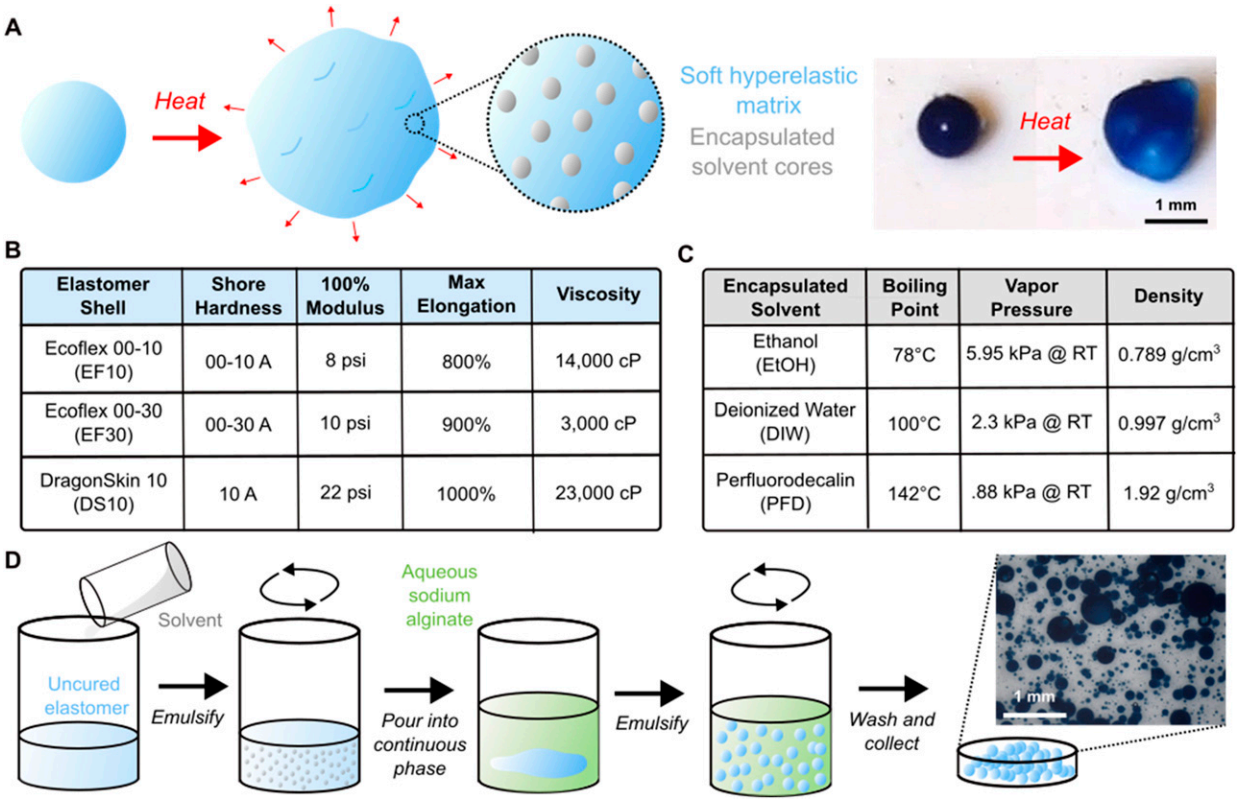

Elastomer Shell	Shore Hardness	100% Modulus	Max Elongation	Viscosity
Ecoflex 00-10 (EF10)	00-10 A	8 psi	800%	14,000 cP
Ecoflex 00-30 (EF30)	00-30 A	10 psi	900%	3,000 cP
DragonSkin 10 (DS10)	10 A	22 psi	1000%	23,000 cP

Encapsulated Solvent	Boiling Point	Vapor Pressure	Density
Ethanol (EtOH)	78°C	5.95 kPa @ RT	0.789 g/cm^3
Deionized Water (DIW)	100°C	2.3 kPa @ RT	0.997 g/cm^3
Perfluorodecalin (PFD)	142°C	.88 kPa @ RT	1.92 g/cm^3

Figure 1. (a) Schematic and demonstration of granular actuators. Granular actuators are capsules that undergo volumetric expansion when heated due to the liquid-to-gas phase change of encapsulated solvent in a soft hyperelastic matrix. (b) Table of material properties of different elastomer shells used in this study. (c) Table of material properties of different encapsulated solvents used in this study. (d) Schematic of double emulsion synthesis method used to create granular actuators.

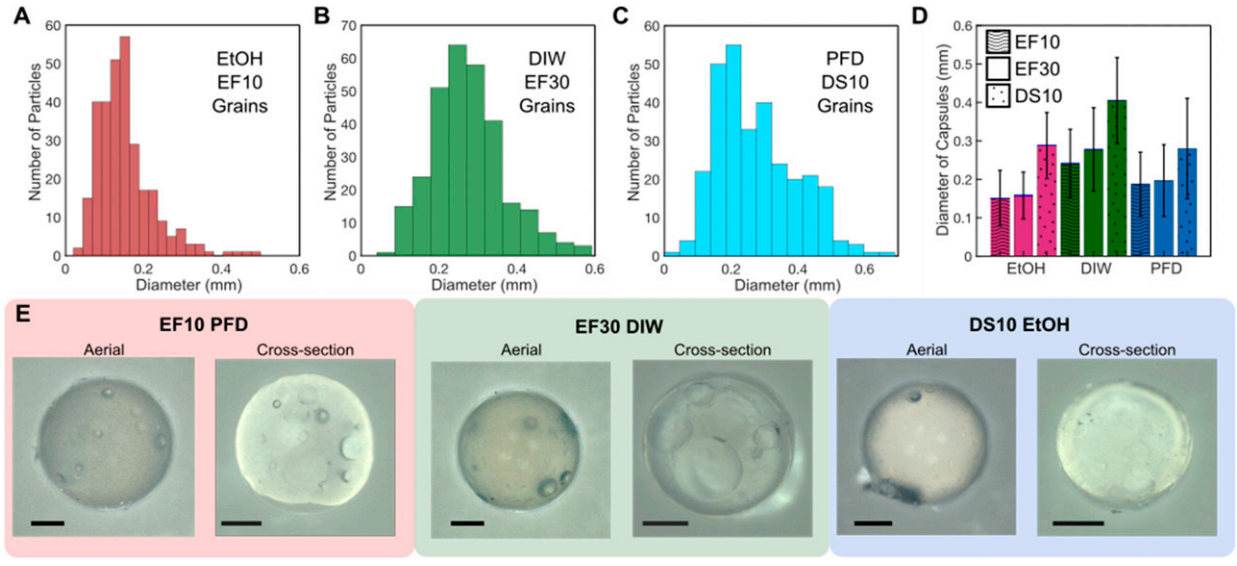

Figure 2. (a) Size distribution of ethanol (EtOH)-encapsulated Ecoflex 00-10 (EF10) grains. (b) Size distribution of deionized water (DIW)-encapsulated Ecoflex 00-30 (EF30) grains. (c) Size distribution of perfluorodecalin (PFD)-encapsulated DragonSkin 10 (DS10) grains. (d) Average diameter of all capsules synthesized and tested. (e) Optical aerial and cross-sectional microscopy images of different grains. All scale bars represent 500 μm.

Figure 2(e) shows physical characterizations of the grains using optical microscopy. The grains exhibit spherical morphologies with very few surface defects, rendering the synthesis procedure successful in synthesizing smooth spherical grains. Additionally, in the cross-sectional optical microscopy images, we see that the grains exhibit an inner structure with multiple cavities, which is presumably where the solvent resides prior to expansion. Different combinations yield different internal morphologies, which may be due to solvent-matrix interactions. For example, there appears to be a large number of pockets in the EF30 DIW grains, meaning that EF30 and DIW may have excellent solvent compatibility.

Encapsulation efficiency

In order to enable successful volumetric expansions of phase-change soft actuators, it is crucial to encapsulate solvent within the hyperelastic matrix. During the double emulsion process, the uncured hyperelastic matrix is not only mixed with the chosen solvent, but also interfaced with an aqueous sodium alginate solution to enable droplet break-up. Therefore, it is critical to ensure the encapsulated material in the grain is indeed the chosen solvent and not any other component of the synthesis method. Thermogravimetric analysis (TGA), wherein the mass of a sample is measured as it is subject to a thermal ramp, was conducted for all grains. By performing TGA on the granular actuators, we can approximate the BP of encapsulated contents in the grains by referring to the temperature range in which the grain experiences mass loss.

Figure 3(a)–3(c) shows TGA curves for all EF10 grains, all EF30 grains, and all DS10 grains, respectively. Grains tested had the same vol.% of solvent encapsulated, nominally 7 vol.%. All results indicate mass decreasing as a function of temperature, which is due to encapsulated solvent evaporation with an increase in temperature. As expected, samples encapsulated with higher BP solvents exhibit mass loss at higher temperatures. Perfluorodecalin (PFD) has a density of approximately twice that of ethanol and deionized water, which is why the mass loss is approximately 2× that of the ethanol and deionized water grains. Figure 3(d) shows TGA curves of all PFD grains. Some differences in the slope of the curves as the samples are reaching the BP of the encapsulated solvent (142°C) are present. This may be due to the material properties of the specific elastomers chosen for this study, where elastomers like EF10 perhaps have less insulating properties or are more porous and thus, cannot prevent solvent escape as effectively when compared to the other studied elastomer shells.

While all the grains in the following characterizations were fabricated with uniform encapsulated solvent vol.%, determining encapsulation efficiency of the different solvent-matrix combinations allows us to further understand solvent-matrix compatibilities and how the synthesis method may affect these results. Figure 3(e)–3(h) shows calibration curves for all sample combinations, with second-order polynomial fittings indicated in the solid lines.

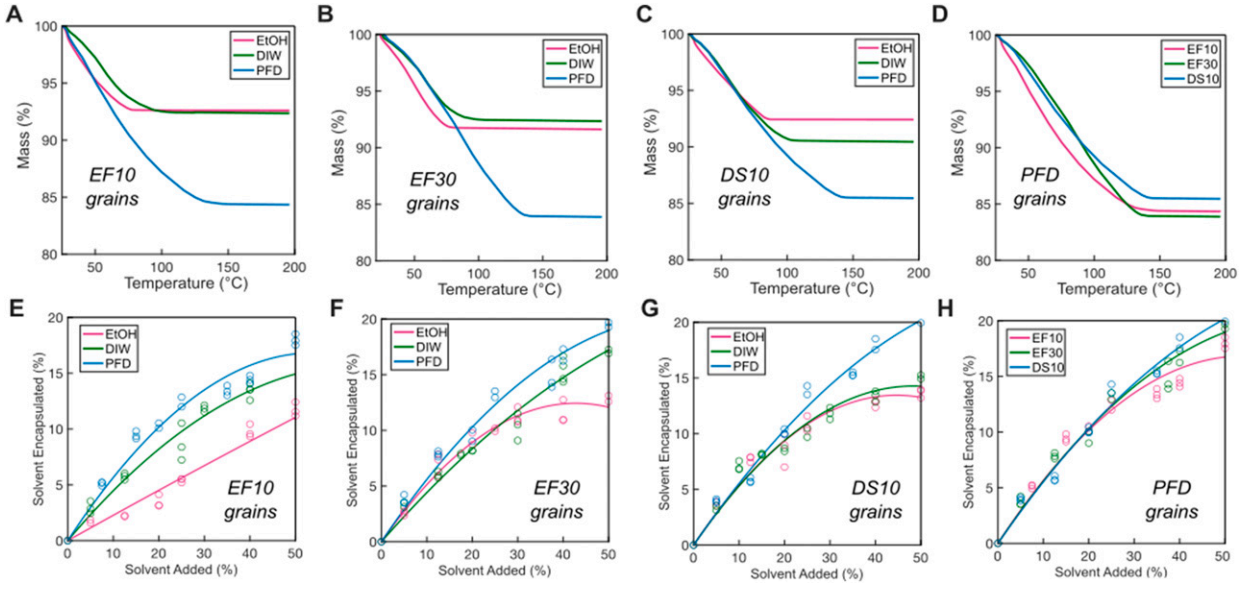

Figure 3. (a) Thermogravimetric analysis (TGA) of all Ecoflex 00-10 (EF10) grains, (b) all Ecoflex 00-30 (EF30) grains, (c) all DragonSkin10 (DS10) grains, and (d) all perfluorodecalin (PFD)-encapsulated grains. (e) Calibration curves with second-order polynomial fittings for all EF10 grains, (f) all EF30 grains, (g) all DS10 grains, and (h) all PFD grains.

Samples were first synthesized and their mass was measured immediately after collection. Thereafter, the grains were left out to dry to allow for solvent evaporation. Each point on the plot corresponds to a group of capsules tested, with multiple groups being tested for different loading conditions. Figure 3(e) shows all EF10 grains, Figure 3(f) shows all EF30 grains, and Figure 3(g) shows all DS10 grains. As expected, there appears to be a slight plateau at higher concentrations of all solvents. Particularly, we see an early plateau for ethanol grains throughout all matrix materials, which may be due to the premature evaporation of EtOH prior to measurement. For DIW grains, we see more encapsulation of solvent compared to ethanol grains, but less than PFD, which also can be owed to the higher compatibility of PFD and PDMS,[25] and also the higher boiling point of PFD, preventing premature solvent escape. We note that the DS10 grains with ethanol and DIW have similar calibration curves, which can provide insight into the material properties of DS10, where the matrix material may have more insulating properties and thus, during synthesis, prevents premature escape of EtOH.

Figure 3(h) shows all PFD grains and their respective calibration curves. It appears that DS10 has the highest encapsulation efficiency, followed by EF30 and finally EF10. This could be attributed to the higher molecular weight of DS10,[26] which may enable greater volumetric encapsulation of the perfluorodecalin. Additionally, the more insulative properties of DS10 may prevent solvent escape over time.[27]

Actuation properties

To determine the actuation properties of the different granular actuators, actuation stress and volumetric expansion measurements of the grains were conducted. Prior work on granular actuators used a dynamic mechanical analyzer (DMA) in a compression iso-strain configuration to determine the actuation stress of the grains. However, due to the limitations of the DMA, the grains could only be thermally ramped at a rate of 20°C/min. This ramp rate is slow, and since grains undergo solvent evaporation during this process, particularly when using low-boiling-point solvents such as EtOH and DIW, a significant reduction in actuation stress was noted. The method used in this study is shown in Figure 4(a), which is able to capture more accurate actuation stress values. First, a modified upper plate is attached to a universal testing system and is lowered to establish a pre-load onto a grain resting on a hot plate. Thereafter, the grain undergoes volumetric expansion and the load cell measures the force exerted on the upper plate. A drawback to this new approach is that all samples are tested at the same temperature, preventing critical data collection on temperature of actuation. Therefore, the use of a DMA is still important in determining key temperature-dependent properties of the actuation of granular actuators.

Figure 4(b) shows the actuation stress results using the method shown in Figure 4(a), with the first bars representing EF10 grains, the middle bars representing EF30 grains, and the last bars corresponding to DS10 grains. We note that generally, the DIW grains exhibit the highest actuation stresses, which may be due to the temperature used for the test (200°C). Since ethanol has a BP substantially lower than the testing temperature, the grain may have undergone solvent evaporation prior to the start of the test. Conversely, since PFD has a BP of approximately 142°C, which is approximately 40°C higher than that of DIW, PFD grains may require more heat to reach critical expansion pressure. Additionally, we note that in general, the DS10 grains exhibit lower actuation stresses for the ethanol and DIW grains. This may be due to the high stiffness of DS10 in comparison to other elastomers used, requiring more internal pressure to induce volumetric expansion. The encapsulated solvent may also escape through the porous silicone shell as pressure builds, reducing the amount of actuation material and resulting in lower registered actuation stress. Finally, the lowest actuation stress measured is the ethanol DS10 grain; a combination of the stiffest grain with the lowest BP encapsulated-solvent makes it difficult to reach critical expansion pressure, as the elastomer requires a significant amount of pressure due to its high stiffness, but the solvent is evacuating the matrix prior to reaching this critical pressure. While the standard deviations among all groups are relatively high, we note clear trends that enable optimizing choice of actuator based on force requirements.

Stress-strain testing was performed to evaluate the stability of the grains under compressive loads, both before and during actuation. Figure S2 shows the passive stress-strain response of grains in their unactuated state. In all cases, the DS10 grains exhibit the highest stiffness, while the EF10 and EF30 grains exhibit similar stiffness under compression. Figure S3 shows the stress-strain response of grains in both unactuated and actuated states. Due to the rapid timescales of actuation, stress data for the actuated state were collected at strain intervals and plotted with polynomial fittings. In all cases, the measured stresses at any given strain are higher for grains in the actuated state compared to the unactuated state. The observed stress trends across all grains align with the findings from the actuation stress testing shown in Figure 4(b), further validating the results.

Despite the shortcomings of using a DMA for analysis of the actuation characteristics of the grains, the method is able to provide key insights into the actuation properties, such as the temperature at maximum actuation. Figures 4(c) and 4(d) show representative actuation stress measurements of all EF10 grains and all DIW grains, respectively. Figure 4(c)

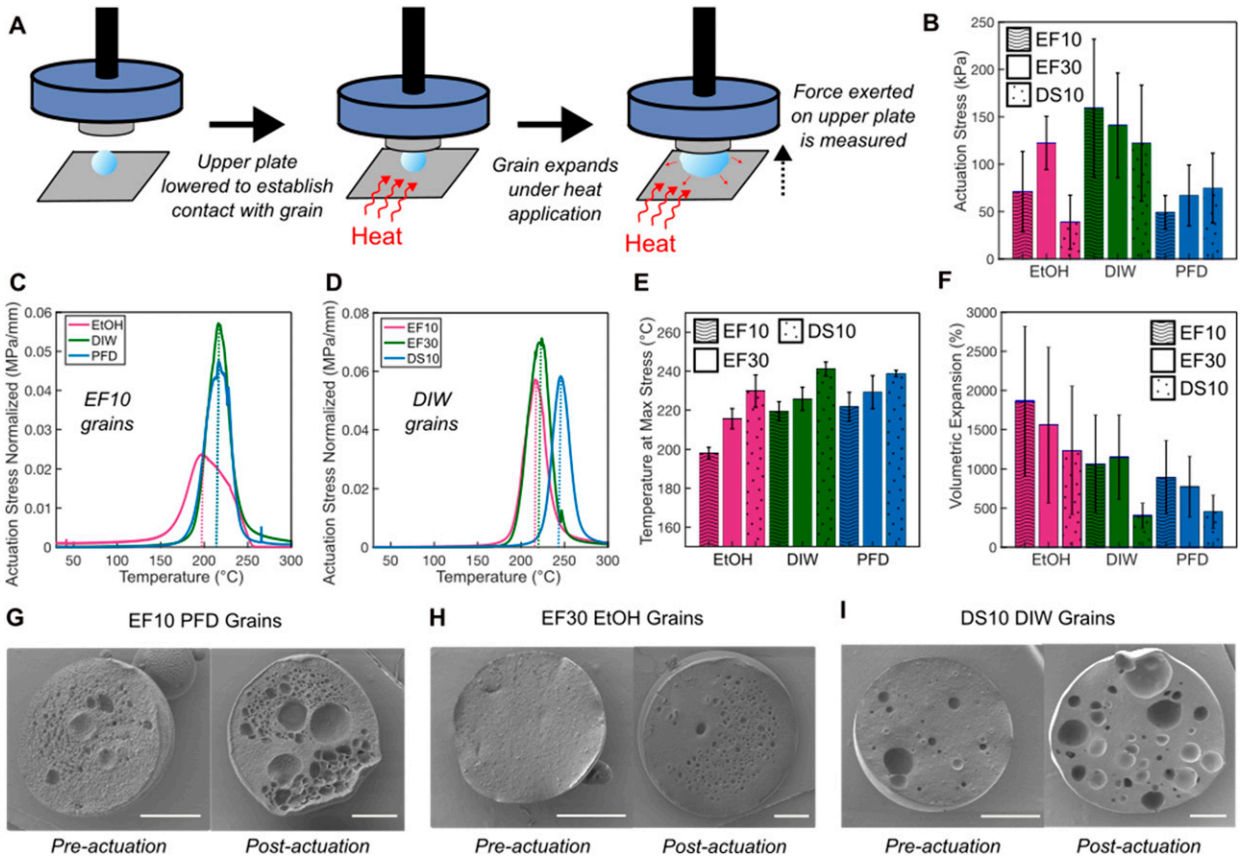

Figure 4. (a) Schematic of test set-up used to capture actuation stress measurements. (b) Actuation stress measurement results taken at 200°C for all grains. (c) Representative actuation stress measurements of all Ecoflex 00-10 (EF10) grains using the dynamic mechanical analyzer. (d) Representative actuation stress measurements of all deionized water (DIW)-encapsulated grains using the dynamic mechanical analyzer. (e) Temperature at maximum actuation stress of all grains. (f) Measured volumetric expansions of all grains. (g) Pre- and post-actuation cross-sectional scanning electron microscopy (SEM) images of an EF10 grain with encapsulated perfluorodecalin (PFD). (h) Pre- and post-actuation cross-sectional SEM images of an Ecoflex 00-30 (EF30) grain with encapsulated ethanol (EtOH). (i) Pre- and post-actuation cross-sectional SEM images of a DragonSkin 10 (DS10) grain with encapsulated DIW. All scale bars represent 500 μm.

highlights the significant reduction in the actuation of ethanol grains in comparison to DIW and PFD grains. This does not match with the data in Figure 4(b), as the temperature of the test is not consistently held at 200°C but is undergoing a temperature ramp of 20°C/min to 300°C. Since ethanol has the lowest BP of the three solvents, it presumably undergoes significantly more evaporation pre-actuation when compared to the other two solvents, explaining the reduction in measured stress. Figure 4(d) shows the actuation stress measurements of different grain combinations yield different temperatures at maximum actuation, allowing one to toggle with the temperature of actuation of the grain based on what constituent materials are chosen.

Figure 4(e) summarizes the temperature at maximum actuation stress (denoted T_A) across all grain combinations, with the first bars corresponding to EF10 grains, the middle to EF30 grains, and the last bars corresponding to DS10 grains. In general, the trend shows an increase in encapsulated solvent BP leads to an increase in T_A, because higher temperatures are required to vaporize solvents with a higher BP. Furthermore, the data shows that the T_A increases as the stiffness of the elastomer matrix is increased (with the lowest being EF10 and the highest being DS10). This is presumably due to an increased required internal pressure in stiffer materials, which is more easily accessible when the ambient temperature is higher and the encapsulated solvent in turn has a higher vapor pressure. The higher T_A of DS10 grains may also explain the lower measured actuation stresses, as a uniform testing temperature was used to assess actuation stresses for all grains.

Volumetric expansion of the grains was determined by placing grains on a hot plate set to 200°C and video recording the free volumetric expansion of the grains. Thereafter, the volumetric expansion was calculated using image analysis, with results being displayed in Figure 4(f).

While the error bars are large, the general trend shows volumetric expansions of ethanol grains being the highest. Furthermore, we see that all DS10 grains have the lowest measured volumetric expansion when compared to other grains, which may be owed to their high stiffness and operation at a suboptimal temperature. Of course, this characterization technique is not perfect, as different grains exhibit maximum actuation stresses, and maximum volumetric expansions, at different temperatures. However, the results provide some insight into which material choices to choose to enhance volumetric expansion at a given temperature.

When grains undergo large volumetric expansions, on the order of several thousand percentages, they inevitably undergo plastic deformation. Although grains do exhibit some shape-recovery post-actuation, returning to a form similar to their initial state as they deflate, they do not fully recover their original shape and size, as measured quantitatively in prior work.[14] In Figures 4(g)–(i), cross-sectional scanning electron microscopy (SEM) images of grains pre- and post-actuation are shown. In all examples, we see that grains exhibit more complex microstructures with higher pore counts post-actuation. The pores pre-actuation are presumably where solvent inclusions reside within the matrix. All grains post-actuation are imaged and shown in Figure S4. The EF10 grains generally exhibit more plastic deformation, likely due to their comparatively low stiffness. Furthermore, the DIW grains show much larger pores than other encapsulated solvents, possibly because the high surface tension of water prevents the formation of smaller, distributed cores, leading instead to larger solvent cores.

Comparison to other soft actuators

Granular phase-change actuators boast high volumetric expansions and rapid response times. To emphasize these advantages, we compare granular phase-change actuators with other phase-change soft actuators. Figure 5(a) presents an Ashby plot of actuation speed (strain rate) versus maximum axial strain. Due to their relatively small size and rapid volumetric expansion, granular actuators exhibit markedly faster actuation speeds compared to other prominent phase-change actuators. Moreover, the maximum axial strains of the granular actuators studied span the full range of those observed in other phase-change actuators, offering the potential for rapid actuation with tunable axial strain.

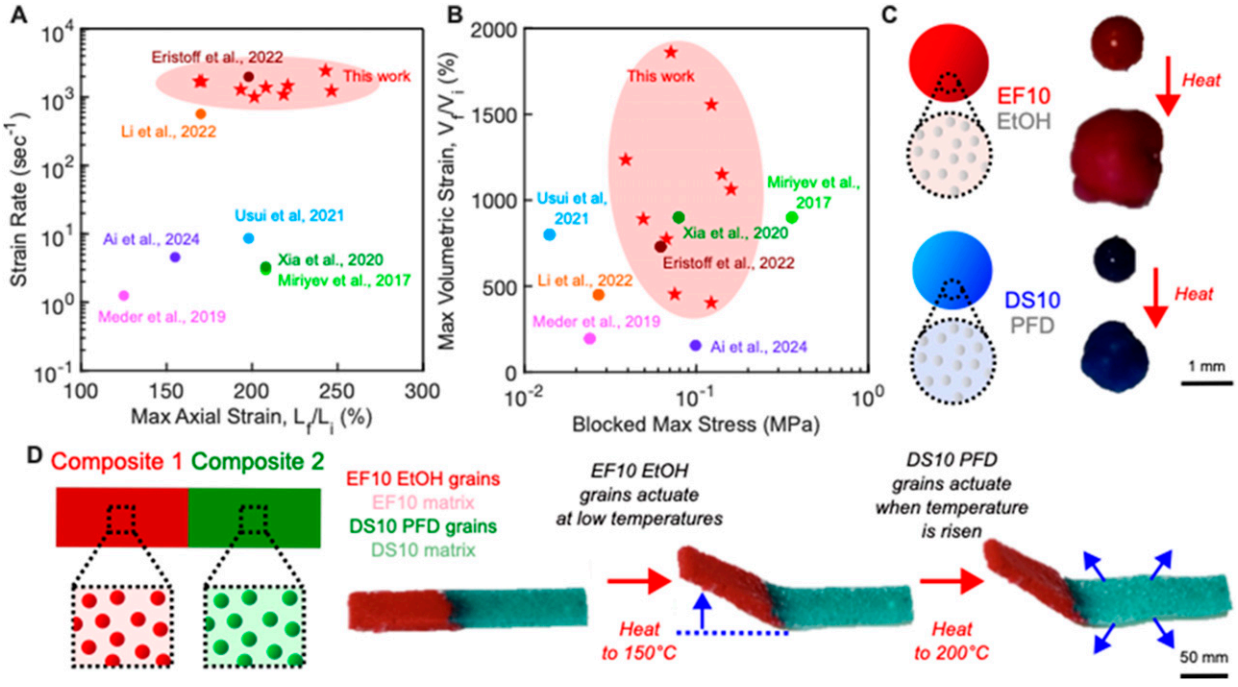

Figure 5. (a) Comparison of normalized actuation speed (strain rate) with respect to maximum axial strain, and (b) Comparison of maximum volumetric strain with respect to actuation performance (blocked stress) of similar phase-change actuators.[14,18,19,21,28–30] (c) Demonstration of two different grains undergoing actuation. The red grain is an Ecoflex 00-10 (EF10) grain with encapsulated ethanol (EtOH) and can undergo larger volumetric expansions. The blue grain is a DragonSkin10 (DS10) grain with encapsulated perfluorodecalin (PFD), and does not undergo as large a volumetric expansion despite being held at the same temperatures. (d) Demonstration of different granular composites actuating at different temperatures. The red EF10 EtOH grains actuate when the material is subject to 150°C, but the green DS10 deionized water (DIW) grains do not. However, when the temperature is raised to 200°C, the DS10 DIW grains begin to undergo volumetric expansion, showcasing the opportunity to utilize different grains for different actuation sequences.

Figure 5(b) displays an Ashby plot of maximum actuation stress versus maximum volumetric strain. Granular actuators generally demonstrate comparable, if not superior, actuation stresses relative to other phase-change actuators. Additionally, their volumetric strains cover a wide range, comparable to those of other phase-change systems. The actuators achieve a range of volumetric strains (403%–1861%) and actuation stresses (38.8–160 kPa), broadening the range of achievable properties for phase-change actuators. Further comparisons between granular actuators and other soft actuators, including shape memory polymers, electroactive polymers, and hydrogels, are provided in Figures S5 and S6.

Demonstrations of different granular actuators

As shown in Figures 3 and 4, grains composed of different material combinations exhibit distinct actuation properties. In Figure 5(c), we compare an EF10 EtOH grain and a DS10 PFD grain actuating under similar conditions (comparable grain sizes, identical volumetric loading of solvent and temperature). However, the DS10 grain undergoes significantly less volumetric expansion when compared to the EF10 grain, which agrees with reported data. This difference can be attributed to the higher BP of PFD and higher stiffness of DS10, making it more difficult to reach its critical expansion pressure. Additionally, Movie S1 shows the expansion of the DS10 grain consists of short and rapid bursts, while the EF10 grain expands more gradually and holds the expanded configuration for longer.

Figure 5(d) demonstrates a bulk composite of grains with varying properties. First, a composite of EF10 EtOH grains in an EF10 matrix was created and attached to a DS10 PFD grain composite in a DS10 matrix. Both composites had similar grain sizes, 50 vol.% loading, and the same volumetric solvent loading. Due to the temperature differences observed in Figure 4 at maximum actuation stress, the two-part composite was subjected to different thermal conditions. Initially, it was heated to 150°C, causing only the EF10 EtOH grains to actuate and rise. When the temperature was increased to 200°C, the DS10 PFD grains began to actuate.

Conclusion

The aim of this study was to explore how key factors influence the synthesis and performance of granular phase-change soft actuators. Our results demonstrate that the choice of constituent materials significantly affects not only the size and internal morphology of the actuators, but also their encapsulation efficiency and various actuation performance metrics. We observed a positive correlation between the stiffness of the elastomer shell and the boiling point of the core solvent with actuation temperature. Additionally, softer elastomer shells were associated with greater volumetric expansions.

Previous research on granular phase-change actuators has not extensively examined the influence of material selection and processing parameters. We studied how encapsulation efficiency varies with different solvent loading volumes, offering insights into synthesis limitations and maximum encapsulation efficiency of up to 20 wt.% for PFD and approximately 15 wt.% for EtOH and DIW. Although we did not directly measure actuation force as a function of encapsulation efficiency, understanding the encapsulation efficiency of different solvents and shell materials will prevent wasteful synthesis processes and allow for optimal mixing ratios.

Granular actuators exhibit immense versatility, where one can use them both individually and in bulk agglomerates to achieve different length-scales of actuation. For example, one can envision using individual grains as micro-actuators, embedding grains in a carrier fluid to deliver actuators to specific locations (for example, hard to reach locations), creating a granular composite to enable 3D printable actuators, and granular actuator assemblies to achieve soft actuators with reconfigurability and active stiffness differentials, as demonstrated in a prior work.[14] Tailoring phase-change granular actuators to specific applications will be essential for their integration into robotic systems. For instance, minimizing actuation temperature will be critical for applications involving living materials, whereas higher actuation temperatures might be more suitable for high-temperature environments where premature activation could be problematic. Understanding how material properties influence key performance metrics, such as actuation temperature, stress, and strain, will aid in selecting the best actuator for each application.

The large standard deviations in some of our measurements, likely due to variability in the synthesis process, suggest that greater synthesis control is needed. We hypothesize that inconsistencies in solvent encapsulation within individual grains could account for the variability in actuation force and volumetric expansion. Future efforts may focus on refining the synthesis process, possibly by employing microfluidic techniques or more complex emulsion techniques, such as in-situ polymerization, to achieve more consistent results. Additionally, because granular actuators experience solvent evaporation after actuation, they cannot undergo repeated actuation. Further work may include increasing cyclic stability of granular actuators via introduction of thermally-conductive fillers, such as those used in Xia et al., to prevent thermal degradation over time.[21] Through the deeper analysis of granular actuator performance presented herein, we aim to establish clear guidelines for materials selection and

synthesis, ultimately enhancing their suitability for a range of applications.

Experimental

Materials

Ecoflex 00-10, Ecoflex 00-30 and DragonSkin 10 were all purchased from Smooth-On (Macungie, PA). Ethanol and perfluorodecalin were purchased from Sigma Aldrich (St. Louis, Missouri). Sodium alginate was purchased from Modernist Pantry (Eliot, ME).

Synthesis of grains

First, a 3 wt.% sodium alginate mixture was created by overhead mixing sodium alginate powder and water for approximately 30 minutes at 500 rpm. Grains were synthesized at room temperature using the double emulsion method outlined in Figure 1(d). Approximately four grams of uncured elastomer was mixed with the desired solvent volume (see calibration curves in Figure 3). The two materials were mixed in a planetary mixer (ARE-310 Thinky) at 1000rpm for 1 min. Thereafter, the mixture was poured into 40 mL of the aqueous sodium alginate mixture and mixed in the planetary mixer for 3 minutes at desired rpm (220-500 rpm). Thereafter, the grains underwent curing over the span of 2 hours at room temperature prior to being washed and filter through a 45 μm ASTM standard sieve. Grains were stored in their respective encapsulated solvents prior to being used, so as to prevent solvent escape over time.

Physical characterization

Optical images were taken using a Zeiss Smart Zoom 5. Cross-sectional scanning electron microscopy (SEM) images were taken using a Hitachi SU-70 at 2 kV. Grain diameters were determined using image analysis techniques on ImageJ.

Materials characterization

Thermogravimetric analysis was completed on a thermogravimetric analyzer (TGA Q550, TA Instruments). The samples were placed in a platinum pan prior to being ramped at 3°C/min in a nitrogen environment. A grain size of approximately 1 mm diameter was used, and the emulsion mixing speed, which determines grain size, remained constant during the corresponding TGA experiments.

Calibration curves were obtained by creating samples and measuring their mass before and after 7 days, in which samples were left out so that the encapsulated solvent would evaporate. A grain size of approximately 100-300 μm diameter was used.

Actuation force measurements were conducted on multiple systems. The first test was conducted on a universal testing system (Instron 3345), using a modified compression fixture. Grains of approximately 1-2 mm in diameter were placed on a hot plate set to approximately 200°C and an upper plate fixture was lowered until a preload of approximately 0.1 N was registered. Thereafter, the grains underwent volumetric expansion and the force on the upper plate was registered and divided by cross-sectional area to provide actuation stress values.

Actuation force measurements to determine temperature of actuation were performed using a dynamic mechanical analyzer (DMA Q850, TA Instruments) with a parallel compression plate fixture of 23 mm in diameter. Composite specimens, where 50 vol.% of grains were embedded in the same shell-material uncured hyperelastic resin, were used because single grain measurements are difficult to successfully complete with the slow thermal ramp rate of the DMA. As single grains are heating, the encapsulated solvent is undergoing evaporation, making it difficult to accurately measure the actuation stress of single grains in this set-up. This test was specifically completed to qualitatively characterize the peak values of the actuation sequences (shape of the curves), as well as characterize the temperature of actuation as the previously mentioned technique utilizes constant temperature values for all specimens. Reported actuation stress values are obtained by dividing the measured force by the cross-sectional area and thickness of the composite sample. Thereafter, the value is doubled to represent that the composite sample only consisted of 50 vol.% capsules.

Specimens were placed into a shallow aluminum dish machined such that the upper compression plate of the DMA fit neatly within its inner diameter. An initial preload of 500 Pa was applied to the specimen prior to starting the isostrain measurement. The temperature of the DMA chamber was then increased to 300°C at a rate of 20°C/min (the fastest thermal ramp rate for the DMA) in nominal air atmosphere. Blocked expansion force was measured as the specimens underwent volumetric expansion. The grain size used for the composite specimens ranged from 1 to 2 mm in diameter.

Stress-strain responses were conducted using a DMA, with a 23 mm diameter compression plate fixture. For the unactuated samples, grains were loaded and subject to a preload of 500 Pa before compression at a rate of 100 mm/min. For the actuated samples, grains were loaded in the same manner and compressed to specific strains (12.5%, 25%, 37.5%, and 50%) at a rate of 100 mm/min. Thereafter, the grains were subject to forced hot air until they actuated, and an actuation stress was registered. The grain size used

for the stress-strain testing ranged from 1.5 to 2.5 mm in diameter.

Volumetric expansions of the grains were measured using image analysis techniques. Grains were placed onto a hot plate measured at 200°C and filmed until expansion. The initial size of the grain was compared to the largest grain size measured. Grain sizes ranging from 1 to 2 mm in diameter were used.

Demonstrations

For the first demonstration, grains were synthesized with a diameter of 1-2 mm and placed on a hot plate measured at 200°C. The grains underwent free volumetric expansions, which were recorded and analyzed.

For the second demonstration, a grain size of approximately 100-300 μm diameter was used. Grains were incorporated into an uncured hyperelastic matrix at 50 vol.% loading and allowed to cure. The composites were attached together to create an actuator with two different actuation sequences based on temperature. The composite was then placed on a hot plate and ramped to 150°C, and then 200°C, to showcase the multiple temperatures of actuation granular actuators can access.

Author Note

Lina Sanchez-Botero is currently affiliated with Department of Radiology, Weill Cornell Medicine, New York, NY, USA.

Declaration of conflicting interests

The author(s) declared no potential conflicts of interest with respect to the research, authorship, and/or publication of this article.

Funding

The author(s) disclosed receipt of the following financial support for the research, authorship, and/or publication of this article: S.E. was supported by the National Aeronautics and Space Administration Space Technology Graduate Research Fellowship under Grant No. 80NSSC21K1269. L.S-B. was supported by the National Science Foundation under Grant No. IIS-1954591.

ORCID iDs

Sophia Eristoff https://orcid.org/0000-0001-7899-3848
Rebecca Kramer-Bottiglio https://orcid.org/0000-0003-2324-8124

Data Availability Statement

The data that support the findings of this study are available from the corresponding author upon reasonable request.

Supplemental Material

Supplemental material for this article is available online.

References

1. Jenett B, Cameron C, Tourlomousis F, et al. Discretely assembled mechanical metamaterials. *Sci Adv* 2020; 6(47): eabc9943.
2. Hemmerle A, Schröter M and Goehring L. A cohesive granular material with tunable elasticity. *Sci Rep* 2016; 6(1): 35650.
3. Nezamabadi S, Nguyen TH, Delenne JY, et al. Modeling soft granular materials. *Granul Matter* 2016; 19(1): 8.
4. Miskin MZ and Jaeger HM. Adapting granular materials through artificial evolution. *Nat Mater* 2013; 12(4): 326–331.
5. Behringer RP and Chakraborty B. The physics of jamming for granular materials: a review. *Rep Prog Phys* 2019; 82(1): 012601.
6. Bi D, Zhang J, Chakraborty B, et al. Jamming by shear. *Nature* 2011; 480(7377): 355–358.
7. Brown E, Rodenberg N, Amend J, et al. Universal robotic gripper based on the jamming of granular material. *Proc Natl Acad Sci U S A* 2010; 107(44): 18809–18814.
8. Corwin EI, Jaeger HM and Nagel SR. Structural signature of jamming in granular media. *Nature* 2005; 435(7045): 1075–1078.
9. Liu AJ and Nagel SR. Granular and jammed materials. *Soft Matter* 2010; 6(13): 2869–2870.
10. Majmudar TS, Sperl M, Luding S, et al. Jamming transition in granular systems. *Phys Rev Lett* 2007; 98(5): 058001.
11. Hu X, Yasa IC, Ren Z, et al. Magnetic soft micromachines made of linked microactuator networks. *Sci Adv* 2021; 7(23): eabe8436.
12. Liu M, Fu J and Yang S. Synthesis of microparticles with diverse thermally responsive shapes originated from the same janus liquid crystalline microdroplets. *Small* 2023; 19(47): 2303106.
13. Liu M, Jin L, Yang S, et al. Shape morphing directed by spatially encoded, dually responsive liquid crystalline elastomer micro-actuators. *Adv Mater* 2023; 35(5): 2208613.
14. Eristoff S, Kim SY, Sanchez-Botero L, et al. Soft actuators made of discrete grains. *Adv Mater* 2022; 34(16): 2109617.
15. Chou HT, Chou SH and Hsiau SS. The effects of particle density and interstitial fluid viscosity on the dynamic properties of granular slurries in a rotating drum. *Powder Technol* 2014; 252: 42–50.
16. Grosskopf AK, Truby RL, Kim H, et al. Viscoplastic matrix materials for embedded 3D printing. *ACS Appl Mater Interfaces* 2018; 10(27): 23353–23361.
17. Ma T, Yang R, Zheng Z, et al. Rheology of fumed silica/polydimethylsiloxane suspensions. *J Rheol* 2017; 61(2): 205–215.
18. Meder F, Naselli GA, Sadeghi A, et al. Remotely light-powered soft fluidic actuators based on plasmonic-driven phase transitions in elastic constraint. *Adv Mater* 2019; 31(51): 1905671.
19. Miriyev A, Stack K and Lipson H. Soft material for soft actuators. *Nat Commun* 2017; 8(1): 596.

20. Miriyev A, Caires G and Lipson H. Functional properties of silicone/ethanol soft-actuator composites. *Mater Des* 2018; 145: 232–242.
21. Xia B, Miriyev A, Trujillo C, et al. Improving the actuation speed and multi-cyclic actuation characteristics of silicone/ethanol soft actuators. *Actuators* 2020; 9(3): 62.
22. Hirai S, Nagatomo T, Hiraki T, et al. Micro elastic pouch motors: elastically deformable and miniaturized soft actuators using liquid-to-gas phase change. *IEEE Rob Autom Lett* 2021; 6(3): 5373–5380.
23. Kim SY, Liu S, Sohn S, et al. Static-state particle fabrication via rapid vitrification of a thixotropic medium. *Nat Commun* 2021; 12(1): 3768.
24. Buckner TL, Farrell ZJ, Nasab AM, et al. Effects of particle size and oxide shell on variable stiffness performance of phase-changing materials. *J Compos Mater* 2023; 57(4): 619–631.
25. Lee JN, Park C and Whitesides GM. Solvent compatibility of poly (dimethylsiloxane)-based microfluidic devices. *Anal Chem* 2003; 75(23): 6544–6554.
26. Jalil R and Nixon J. Microencapsulation using poly (L-lactic acid) III: effect of polymer molecular weight on the microcapsule properties. *J Microencapsul* 1990; 7(1): 41–52.
27. Huang Y, Wen W, Mukherjee S, et al. High-molecular-weight insulating polymers can improve the performance of molecular solar cells. *Adv Mater* 2014; 26(24): 4168–4172.
28. Ai W, Hou K, Wu J, et al. Miniaturized and untethered McKibben muscles based on photothermal-induced gas-liquid transformation. *Nat Commun* 2024; 15(1): 1329.
29. Li J, Mou L, Liu Z, et al. Oscillating light engine realized by photothermal solvent evaporation. *Nat Commun* 2022; 13(1): 5621.
30. Usui T, Ishizuka H, Hiraki T, et al. Fully flexible liquid-to-gas phase change actuators with integrated liquid metal heaters. *Jpn J Appl Phys* 2021; 60(SC): SCCL11.